Progress in Additive Manufacturing
https://doi.org/10.1007/s40964-025-01053-0

FULL RESEARCH ARTICLE

# Impact of powder bed fusion printing process parameters on the achieved quality of PA12 manufactured parts

**Richard Joch[1] · Michal Šajgalík[1] · Mário Drbúl[1] · Dagmar Měřínska[2] · Jaromír Markovič[1] · Andrej Czán[1]**

Received: 16 September 2024 / Accepted: 1 March 2025


**Abstract**

The study investigates the impact of process parameters in the additive manufacturing technology of powder bed fusion on the properties of manufactured parts. Through experimental analysis, we examine the impact of layer height, laser power, chamber temperature, and sample positioning on surface roughness, tensile strength, and various geometric and dimensional parameters. The samples fabricated from PA12 material are produced using the Sinterit Lisa device, which offers specific parameter adjustment capabilities but lacks precise value setting. The subsequent experimental phase consists of nine carefully designed experiments employing the Taguchi method. We used regression analysis to quantify the impact of individual process factors. Our results reveal significant effects of parameter variations on the final quality of printed objects. Furthermore, these results also underscore the critical importance of model orientation within the printing chamber, influencing achieved tensile strength, surface roughness, and roundness geometric properties. Notably, laser power has a notable impact on the dimensional accuracy of manufactured parts. However, according to our findings, it does not affect surface roughness. Moreover, we observe that laser power, when coupled with chamber temperature, influences the achieved strength of the examined samples. The optimization of these parameters holds promise for enhancing the mechanical properties, geometric properties as well as better surface quality of the final samples. This study offers valuable insights into understanding the laser sintering process better and provides practical guidance to optimize the production process based on this additive manufacturing technology.

**Keywords** PA12 · Surface roughness · Strength · Roundness · Accuracy

## 1 Introduction

Additive manufacturing is applied across a wide range of applications, from prototyping to functional component production [1]. This manufacturing technology comprises seven fundamental types, each directly describing the layer deposition process. According to ISO 17296–2 standards, the seven basic types are considered:

- Vat photopolymerization
- Material jetting
- Binder jetting
- Powder bed fusion
- Material extrusion
- Direct energy deposition
- Sheet lamination

While considerable research exists on the effects of individual powder bed fusion parameters on part properties,

✉ Richard Joch
richard.joch@fstroj.uniza.sk

Michal Šajgalík
michal.sajgalik@fstroj.uniza.sk

Mário Drbúl
mario.drbul@fstroj.uniza.sk

Dagmar Měřínska
merinska@utb.cz

Jaromír Markovič
jaromir.markovic@fstroj.uniza.sk

Andrej Czán
andrej.czan@fstroj.uniza.sk

1 Department of Machining and Production Technologies, Faculty of Mechanical Engineering, University of Žilina, Univerzitná, 8215/1, 010 26 Žilina, Slovakia

2 Department of Production Engineering, Faculty of Technology, Tomas Bata University in Zlín, Zlín, Vavreckova 5669, 76001, Czech Republic

Published online: 15 March 2025

there remains a significant gap in understanding the complex interplay of these parameters. Much of the existing literature focuses on optimizing individual parameters in isolation, often neglecting the synergistic or antagonistic effects that can arise when multiple parameters are varied simultaneously. This research aims to bridge this gap by systematically investigating the combined influence of specimen orientation, laser power, layer thickness, and chamber temperature on the surface roughness, tensile strength and dimensional and geometric accuracy of selective laser sintering produced parts. By employing a design of experiments approach, this study will provide a comprehensive understanding of the parameter interactions and their relative importance in determining surface finish. The findings will contribute to the development of predictive models and optimized processing strategies for achieving desired quality in SLS, ultimately leading to improved part quality and functionality. This research is crucial for advancing the understanding and control of SLS processes, enabling the production of parts for a wider range of applications.

### 1.1 Selective laser sintering (SLS)

Selective laser sintering (SLS) technology employs the selective sintering of material, which is in the form of powder. The manufacturing process involves gradual layering of the powdered material, followed by laser sintering to achieve the desired shape [2]. This process is initiated by adding base layers of powdered material, uniformly distributed onto the build platform using a sliding ruler or a sliding rotary roller to ensure even powder layer application [1]. The radiant heaters then elevate the powder to a temperature below its melting point. The laser melts the required geometry onto the powder layer through a set of scanner mirrors. This makes the individual powder particles fuse within and to the lower layer. The unsintered powder stays in the build chamber and serves as a support material [3]. Once the entire geometry of the layer is sintered, the build platform is moved by one layer height, and a fresh layer of powdered material is applied. This layer-by-layer process continues throughout the manufacturing procedure. The commonly used materials include polyamides (nylon—PA) [4], polypropylene (PP), polylactide (PLA) [5–9], polyetherketoneketone (PEKK) [10–12], and various thermoplastic elastomers. These base materials are frequently enhanced with fillers like carbon fibers (CF), glass beads, or aluminum powder (Alumide) [10, 13]. When using specific materials, the device chamber must be filled with an inert gas, typically nitrogen, to avoid material oxidation [14].

Selective laser sintering devices utilize different types of lasers to melt materials. The laser serves as the energy source for sintering the powder material. Typical SLS printers use $CO_2$ lasers (EOS P110), with powers ranging from 10 to 100 watts, depending on the material and application. For instance, Sintratec S1 use blue diode or the Sinterit Lisa employs a 5-W diode laser [15]. Low-power lasers like the 5-W diode in the Sinterit Lisa are suitable for smaller build volumes and polymers. The Sinterit Lisa has a build volume of $150 \times 200 \times 150$ mm. It offers a layer height that ranges from 0.075 mm to 0.175 mm. To effectively absorb energy from the laser and start the melting process, it is crucial to use a dark pigment in the powder. Since we were unable to directly adjust the scan spacing and roller speed on the system, we concentrated on investigating changes in the power ratio, layer height, and temperature offset. The Laser Power Ratio is a parameter in Sinterit Lisa 3D printing that adjusts the laser's power output relative to its maximum capacity. It represents a percentage or ratio of the laser's full power that is applied during the sintering process. This parameter enables fine-tuning the energy delivered to the powder bed. A higher Laser Power Ratio means more energy is applied, which may be necessary for sintering denser or higher-melting-point materials. Conversely, a lower Laser Power Ratio reduces energy to prevent overheating, which can be beneficial when printing with sensitive or lower-temperature materials.

### 1.2 Impact of parameters

Sintering of powdered material is a process involving fusion and subsequent cooling, influenced by several factors. Laser power, scanning speed, layer thickness, and heating temperature are key properties of SLS technology. The temperature of preheating, powder bed, and sintering impacts the porosity of sintered samples. Several scientific studies focused on the impact of process parameters.

Sachdeva investigates the impact of selective laser sintering process parameters on the surface roughness of parts manufactured with Duraform polyamide. Duraform PA is a nylon-based thermoplastic powder material commonly used in selective laser sintering 3D printing. The authors measured three roughness parameters: Ra (arithmetic mean deviation), Rz, and Rq. They experimented with different parameter settings, keeping the hatch pattern along the X-direction and using a 70/30 ratio of used to virgin powder. The study found that laser power significantly influences surface roughness [16]. Faraj et al. explores the optimization of selective laser sintering parameters for PA12 samples using the Taguchi method. The study focuses on minimizing surface roughness, a key quality characteristic in SLS parts. The authors investigated the influence of laser power, scanning speed, layer thickness, and scanning space, printing samples at different orientations 0°, 45°, and 90°. They developed regression equations for each orientation, establishing a linear relationship between roughness and the studied parameters [17]. Negi et al. in investigated the surface roughness of glass-filled polyamide parts fabricated using selective laser sintering finish [18]. They used a face-centered central composite design of experiment, varying five key parameters: bed temperature, laser power, scan speed, scan spacing, and scan length. Their analysis, using response surface methodology, revealed that scan spacing followed by laser power were the most significant factors influencing surface roughness. They also determined optimal parameter settings for achieving improved surface. Nar et al.'s research underscores the complex interplay of factors affecting surface roughness in selective laser sintering processes [19]. Their findings stress the need to carefully control processing parameters and consider part orientation to achieve the desired surface quality. The study found that higher energy density produced smoother surfaces, aligning with the expectation that increased energy leads to more effective powder melting and fusion. Additionally, the researchers noted that roughness varied across the powder bed, with edges and corners exhibiting higher roughness than the center, suggesting potential inconsistencies in the laser's energy distribution or powder bed temperature distribution across the build platform. Khademe Razaviye et al. investigated the mechanical properties (strength, modulus of elasticity, and elongation) of PA12 parts, specifically PA2200, produced by SLS 3D printing [20]. They focused on the effects of laser power, scan speed, hatch spacing, and scan length. Laser power and scan speed play significant roles. Higher laser power and lower scan speed generally improve mechanical properties, but excessive power can lead to part defects. Laser energy density is a crucial parameter. Higher energy density, achieved through a combination of higher laser power, lower scan speed, and smaller hatch spacing, results in stronger parts.

Laser power is a crucial parameter in the powder bed fusion process. Higher laser power increases the energy input, leading to better melting and fusion of the powder particles. This generally results in improved mechanical properties like tensile strength [17] and a smoother surface finish [18, 21]. However, excessive laser power can cause overheating, part defects, and unwanted thermal deformations. Layer thickness also plays a significant role. Thinner layers generally result in better surface finish and resolution but increase build time [22]. Conversely, thicker layers can reduce build time but may compromise surface quality [19]. The orientation of the part within the build chamber affects the support structures required, the direction of the laser scanning, and the resulting mechanical properties. Maintaining a stable and appropriate chamber temperature is crucial for consistent part quality and minimizing thermal stresses. It is important to note that these parameters interact in complex ways. For instance, the optimal laser power depends on the scan speed, scan spacing, and the material being used [19]. Achieving the desired part quality requires careful consideration and optimization of all relevant parameters.

### 1.3 Powder quality

Powder quality plays a crucial role in determining the final properties of SLS parts, impacting not only surface roughness but also tensile strength, dimensional accuracy, and geometric fidelity [23, 24]. Variations in powder characteristics, arising from factors like recycling and aging, can significantly influence these outcomes. The particle size distribution, particle shape, and powder flowability all affect the packing density and thermal behavior of the powder bed, which in turn impacts the sintering process [25].

These material effects, particularly the increase in melt viscosity, also result in an undesired surface finish effect, known as orange peel, following prolonged powder aging [26]. The input material of additive manufacturing also influences the resulting quality of manufactured parts. A distinction arises when using virgin powder and recycled powder [22]. Zarringhalam proved that virgin powder and recycled powder lead to different results regarding elongation at break (EaB) and tensile strength [27]. Recycled powder leads to an EaB of 36–94% depending on the powder manufacturer. This variation could be attributed to different additive manufacturing machines, process parameters, and powder grain sizes. Powder quality was also investigated by Dadbakhsh, who examined virgin powder, recycled, and aged powder material [28]. The results showed that virgin powder sintered and fused fast when heating, while aged powder needed a longer time or higher temperature to reach grain fusion. Recycled powder material exhibited properties between those of virgin and aged powder. Changes in temperature behavior and microstructure resulting from aging influenced densification and laser consolidation. Powder aging increased the molecular weight/length and viscosity due to the post-condensation phenomenon. Dumanhuri also confirmed the presence of voids in the particles of recycled powder. Virgin and aged powder demonstrated a thicker microstructure and had improved bonding quality due to homogeneous crystallization [28]. PA12 powder used in SLS technology can also be reformed into filament [29].

### 1.4 Surface

Fresh, virgin powder typically leads to smoother surfaces due to its consistent particle size distribution and lack of contaminants. Recycled powder, while more economical, can contain partially sintered or degraded particles, leading to increased surface roughness. Similarly, aged powder, exposed to moisture and oxidation, can exhibit altered flowability and melting behavior, further contributing to a rougher surface finish mentions that surface roughness is a major drawback of SLS technology and can be attributed to partial fusion of powder grains [17]. Researchers have recommended optimizing process parameters like laser power, scan speed, and layer thickness to minimize surface roughness and improve the overall part quality produced by powder bed fusion techniques [30, 31].

Surface roughness serves as a qualitative evaluation of the surface quality of a component concerning its previous manufacturing technology. Surface roughness is defined as the sum of irregularities and protrusions over a specific measured length or area [32]. Multiple surface properties can be evaluated over the measured length, but, in practice, the most used parameters are the arithmetic mean deviation of the surface, Ra, and the arithmetic average of the highest profile peaks, Rz. Undesired parameters such as waviness, and component shape change also contribute to the surface measurement, often filtered during measurement [33].

Measurement devices for gaining parameters on surface roughness can be divided into two main groups: tactile and optical measuring methods [34]. The tactile measuring method in determining the roughness of surfaces is one of the predominant methods [35]. The key principle involves acquiring the surface structure using a device equipped with a probing tip of a small diameter, usually 2 µm to 10 µm, directly connected to a sensor [36]. As the tip moves across the surface, the deflection of the tip relative to the sensor changes, resulting in a variation in the initial value of the sensor. The measured data are these changes in values, and they are sent to a computational unit, which processes them to get direct data on the roughness of the surface. A drawback of this method is the tip diameter, which works as a mechanical filter and causes data distortion.

The optical measurement method relies on the concept that a surface consists of phase inhomogeneities. When a beam of light hits such a surface, interaction occurs, followed by the reflection of rays. Depending on the sensing principle, a particular non-contact method is categorized as optical, electron, laser, or ultrasonic [37]. The prevailing type of non-contact measurement method is optical scanning, wherein the measurement result provides the topography of a specific surface, enabling subsequent evaluation of surface roughness.

# 2 Methodology

## 2.1 Sinterit Lisa additive device

The Sinterit Lisa is a compact additive manufacturing machine that utilizes selective laser sintering (SLS) technology to create 3D parts directly from powdered polymers. This equipment is specifically optimized for processing materials like polyamides (PA12) and elastomers (TPU). Its compact design and relatively low operating costs make it ideal for research purposes, prototyping, and small-batch production.

The Lisa is controlled using Sinterit Studio software, which allows users to set up slicing and select various process parameters. The laser power ratio of the Sinterit Lisa refers to the intensity setting of the laser beam relative to its maximum possible power. This setting is essential for effectively bonding the powder material during the selective laser sintering (SLS) process. Optimizing the laser power ratio in SLS technology helps achieve an ideal balance between adequate powder sintering and minimizing the risk of overheating or degrading the material. Layer height is an important parameter in additive manufacturing, as it defines the thickness of each layer of material deposited during the process. Specifically, the layer height indicates the thickness of the powder material that is laser sintered in one step, prior to the application of the next layer. The device allows for a layer height selection ranging from 0.075 mm to 0.175 mm. The Sinterit Lisa features a temperature offset parameter that enables adjustments to the print chamber temperature during the selective laser sintering (SLS) process. This parameter helps correct discrepancies between the set temperature and the actual temperature achieved, ensuring conditions for sintering the powder material. The temperature offset is configured in the Sinterit Studio software and represents the amount by which the actual temperature in the printing chamber should differ from the preset value. Adjustments are typically made in small increments (e.g., ± 2 °C) and are influenced by the specific material used and the printing conditions.

## 2.2 Specimens description

Material tensile strength is the maximum load a material can withstand before breaking when subjected to tension. The static tensile test is precisely defined in standards, which independently describe the test procedure and test samples for different types of materials. During the test, the relationship between the applied force F and the elongation of the test sample is examined on a circular or rectangular cross-section tested sample as the stress–strain relationship until sample failure. The output comprises a graph illustrating the stress–strain relationship, accompanied by stress and strain characteristic values.

Qualitative and strength properties in additive manufacturing are strictly evaluated based on specific standards that describe the shapes of the tested samples as well as their evaluation. Standard STN EN ISO 527–2 is the fundamental norm determining the shapes of test samples for plastics to obtain material strength properties through static tensile testing. According to standard STN EN ISO 527–2, we will use sample 1BA (Fig. 1) for static tensile tests, due to limitations in the working space of the device.

Standard STN EN ISO ASTM 52902:2019 describes test artifacts for evaluating the geometric properties of additive

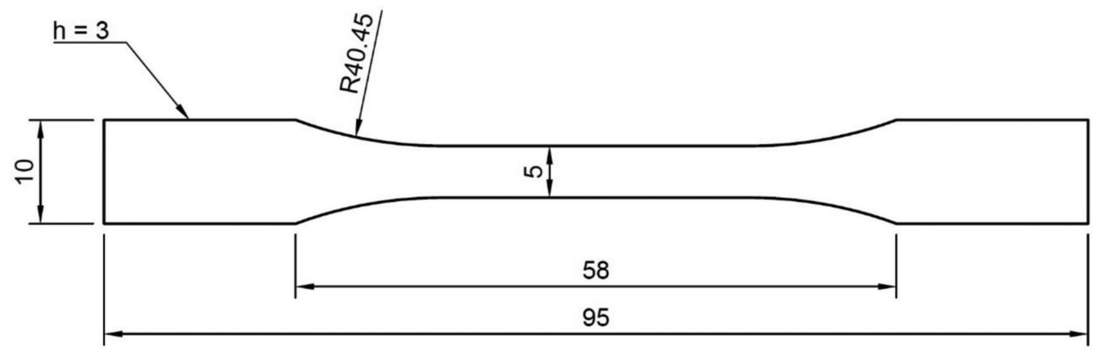


**Fig. 1** Test specimen for tensile testing STN EN ISO 527–2

**Fig. 2** Sample for evaluating circular artifacts according to STN EN ISO ASTM 52902:2019 in additive manufacturing

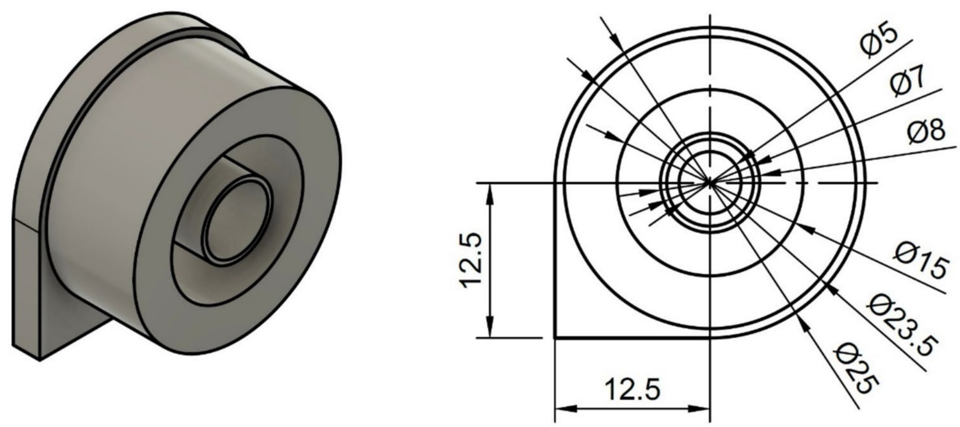


manufacturing systems. The standard includes various bodies allowing the evaluation of diverse geometric properties. To maximize the use of the device's working volume, samples were chosen from standard STN EN ISO ASTM 52902:2019 (Fig. 2). These samples serve as the basis for evaluating the fundamental accuracies of the Sinterit LISA device. More specifically, samples were selected to evaluate circular artifacts (fine size), enabling the evaluation of geometric properties like roundness and dimensional properties like diameters Table 1.

**Table 1** Specification of Sinterit Lisa [38]

| Laser type | IR laser diode 5W |
|---|---|
| Max print volume | PA: 110×160x130 mm<br>TPU: 110×160x145 mm |
| Size of Print Bed | 150×200x150 mm |
| Min. wall thickness | From 0.4 mm |
| Hole diameter | From 0.5 mm |
| Moving part clearance | From 0.2 mm |
| Max temperature in the chamber | 210 °C |
| Average power consumption | 0.9 kW |
| Max power consumption | 1.6 kW |
| Powder profiles | PA12 Smooth, Flexa Gray |
| Dimensions | 620×400x660 mm |

### 2.3 DoE

The software "Sinterit Studio Basic 2019" for the Sinterit LISA additive device includes only three adjustable parameters: layer height [mm], laser power ratio, and chamber temperature deviation [°C]. These three parameters determine the fundamental factors affecting the resulting sample quality. Another factor being investigated is the orientation of the samples within the working volume. However, this factor is not explicitly included in the experiment design because orientations will be encompassed in each sub-experiment. The experimental design is conducted within the Minitab software environment, which offers a range of methods for designing experiments. We need to design the experiment to minimize the number of trials while reducing variability in the dataset. This condition is mainly kept for economic reasons but also due to material limitations for additive manufacturing. The experimental design using the Taguchi method employs an orthogonal arrangement to estimate the impact of individual factors on a specific average response value. Due to its orthogonality, the design is balanced, ensuring that each factor carries equal weight without influencing each other. A 3-factor, 3-level experiment was designed in Minitab, and its details are presented in Table 2. In total, 9 sub-experiments will be conducted, encompassing all necessary combinations of factors and determining the individual impacts of the experiment.

An additional fourth factor, not directly accounted for in the Minitab software design, is the orientation of the samples. By varying the orientation of the samples, we can observe how the orientation affects their geometric properties, including surface roughness and mechanical properties. For tensile test samples, the orientation was designed to rotate the samples around each axis, namely X, Y, and Z (Fig. 3). An angular spacing of 22.5° between each sample was chosen because it offers most effective results while minimizing the number of samples needed and minimize variability between specimens.

The samples for investigating circular artifacts are designed in only three orientations due to their bulkiness and the brittleness of the thin-walled inner cylinder. The base orientation aligns along the X and Y axes, with the cylinder's center along the Z-axis. Subsequent rotations around the X-axis with angular spacings of 45° and 90° relative to the base sample result in two additional sample orientations (Table 3).

**Table 2** Experiment design and individual process parameters

| Experiment No | Layer (mm) | Laser ratio | Temperature offset (°C) |
|---|---|---|---|
| Exp_1 | 0.1 | 1.2 | 0.5 |
| Exp_2 | 0.1 | 1.6 | 2 |
| Exp_3 | 0.1 | 0.8 | −1 |
| Exp_4 | 0.125 | 1.2 | 2 |
| Exp_5 | 0.125 | 0.8 | 0.5 |
| Exp_6 | 0.125 | 1.6 | −1 |
| Exp_7 | 0.175 | 0.8 | 2 |
| Exp_8 | 0.175 | 1.2 | −1 |
| Exp_9 | 0.175 | 1.6 | 0.5 |

**Table 3** Orientation of individual specimens for tensile test

| Specimens | X (°) | Y (°) | Z (°) |
|---|---|---|---|
| A | 90 | 0 | 0 |
| B | 67.5 | 0 | 0 |
| C | 45 | 0 | 0 |
| D | 22.5 | 0 | 0 |
| E | 0 | 0 | 0 |
| F | 0 | 22.5 | 0 |
| G | 0 | 45 | 0 |
| H | 0 | 67.5 | 0 |
| I | 0 | 90 | 0 |
| J | 90 | 90 | 22,5 |
| K | 90 | 90 | 45 |
| L | 90 | 90 | 67.5 |
| M | 90 | 90 | 90 |

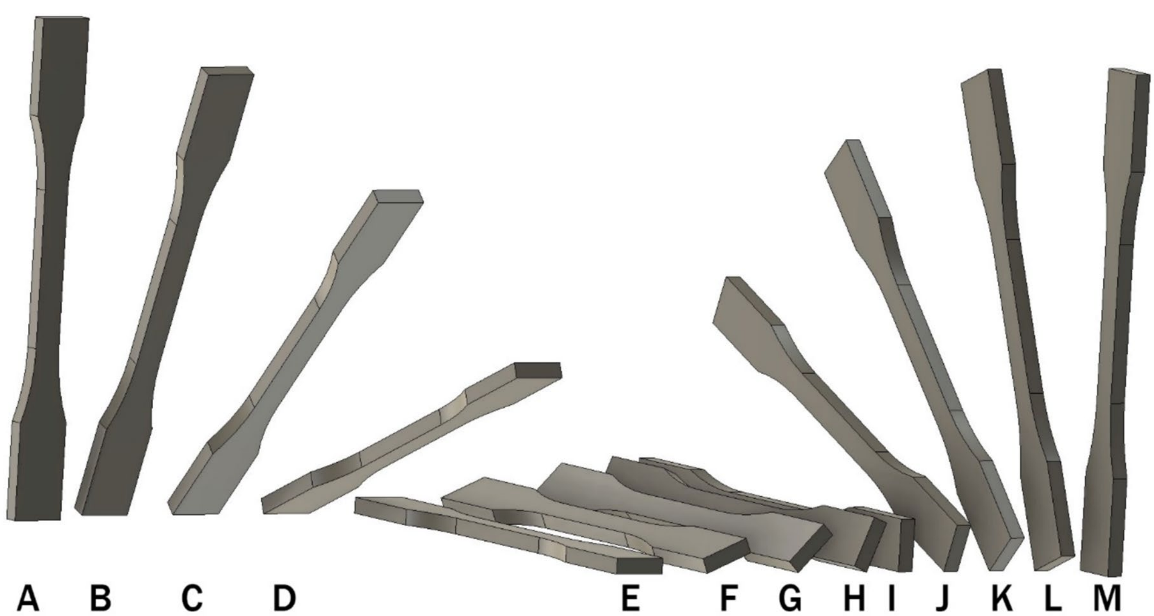


**Fig. 3** Visualization of the proposed specimens' orientations for tensile test

### 2.4 Material for SLS

The material chosen for producing samples for the experiment was PA12 Smooth (Table. 2), directly sourced from Sinterit, the manufacturer of the LISA device. PA12 Smooth is a thermoplastic polymer based on polyamide in powder form, suitable for SLS additive manufacturing [39]. It possesses mechanical properties optimal for the basic prototyping of functional components [40]. Furthermore, according to the manufacturer, this material is known for providing one of the best surface resolutions available.

The material is supplied in two versions v1 and v2, which have different refresh ratios of thermally affected material to pure, unaffected, or new “virgin” material. The experiment focuses on the newer version, v2, where the manufacturer specifies a mixing ratio of 22% with the new material. It is essential to mix a certain amount of pure powder into the thermally affected powder to restore mechanical properties, even after several cycles of thermal influence (Table 4).

**Table 4** Material specification based on manufacturer [41]

| Material type | Nylon 12 | |
|---|---|---|
| Need for nitrogen chamber | No | |
| Refresh ratio | 22% | |
| Color | Navy gray | |
| Particle size | 19–90 µm | *ISO 13320* |
| Nominal particle size | 38 µm | *ISO 13320* |
| Print density | 0,95–0.97 g/cm$^3$ | *PN-EN ISO 845:2010* |
| Melting point | 185 °C | *PN-EN ISO 11357–3:2018* |

### 2.5 Manufacturing preparation

The preparation for manufacturing has several stages. It commences with the generation of 3D models of the samples, followed by their placement in the working space of the device, and ends with the generation of the NC code for the device.

The first main stage involves creating 3D models, which are developed according to the standards STN EN ISO 527–2 and STN EN ISO ASTM 52902:2019. The resulting 3D models are then aligned at certain angles in the CAD software according to the experimental design. Finally, individual 3D models of the samples are exported in the correct orientation.

In the secondary stage, the 3D models are imported into the slicing software, Sinterit Studio 2019. Here, the placement of all samples is designed to maximize the use of the device’s working volume (Fig. 4).

The rest of the preparation involves setting the desired parameters based on the proposed experiment parameters and generating a sliced file directly for the Sinterit LISA printer. During program generation, the software calculates the amount of material needed to be inserted into the chamber, how much virgin material needs to be mixed with the material from the device after production, as well as data on heating time, the length of the production process, and an approximate cooling time for the working space after production. The placement and

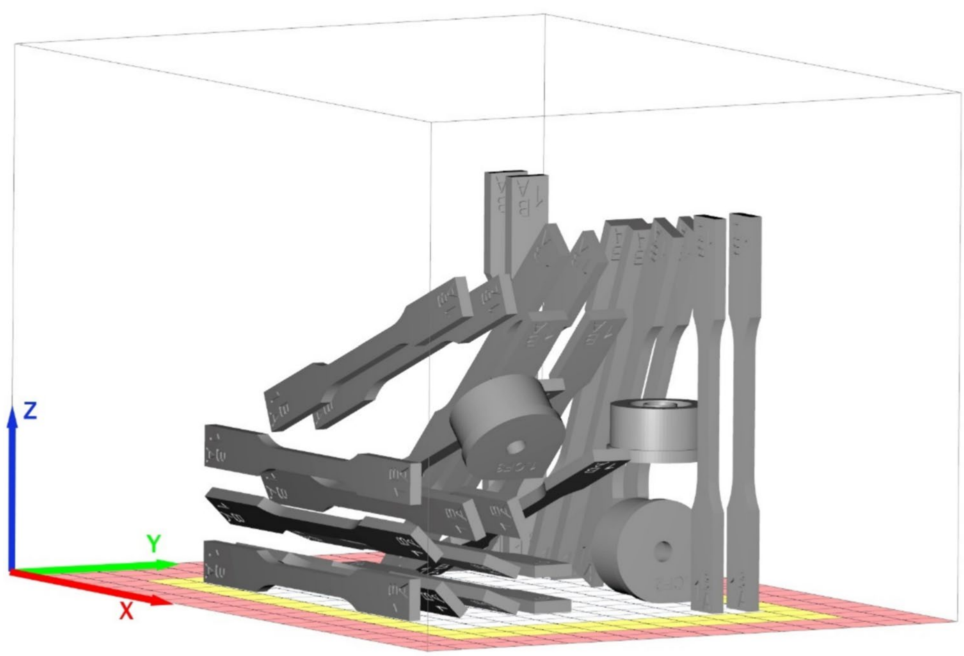


**Fig. 4** Setup of specimens in the Sinterit Studio 2019

orientation of samples in the working space are identical for all sub-experiments.

### 2.6 Measurement methodology

For evaluation, the roughness parameter Rz values were measured for each sample, averaged from four measurements. Rz was chosen due to its higher significance in polymer components. The Rz roughness parameter is a measure of surface roughness that quantifies the height difference between the highest peak and the lowest valley within a specified sampling length. The surface roughness data involved measuring the roughness of each manufactured sample. The measurements were conducted using an optical measuring instrument, Alicona InfiniteFocus Each specimen was securely clamped in a fixture, and four measurements were conducted on every specimen. The measurement locations were on the wider surface of the specimen and were recorded along its length. For sample E, the upper surface was measured. This surface had been marked and identified on the model prior to the experiment. When the samples were oriented for testing, the same predetermined surface was consistently measured, such that if a sample was rotated by 90° within the machine coordinate system, the measured surface became the side surface rather than the originally marked upper surface.

The mechanical properties were tested using a tensile testing machine from Zwick. All samples were tested under the following conditions: the distance between the movable jaws was 50 mm, and the speed was 50 mm/min for all samples. The temperature was maintained at 23 °C. The test was conducted according to ISO 527–3 standard.

Geometric properties such as roundness and cylindricity were measured using a CMM machine Zeiss Eclypse, with measurement programming and evaluation conducted through Zeiss Calypso 7.3. Each circular sample was measured, with each measured feature evaluated using three circular paths spanning 380° angularly. Based on the model dimensions, a measurement speed of 3 mm/s was selected for diameters D23 mm and D15 mm, with a step size of 0.1. For smaller diameters D8 and D7, a measurement speed of 2 mm/s and a step size of 0.05 were chosen. A measuring ruby touch probe with a diameter of 1.5 mm was selected for the groove between the measured features of the model, spaced at a distance of 3.5 mm. Based on the measurements of circular paths, the values for four sample diameters were gained, derived from circular paths in the middle section of the measured sample and evaluated using the Gaussian method, commonly used for process monitoring. The minimum element method was employed as the roundness evaluation method.

## 3 Results

The presented results are gained through the measurement and analysis of samples achieved through experimental activities.

### 3.1 Surface

To comprehend the impact of individual parameters on the resulting surface roughness of the samples, we constructed a Pareto chart of effects (Fig.7). The Pareto chart presents the absolute values of standardized effects arranged from the largest to the smallest. It also includes a reference line that indicates which effects are statistically significant. The position of this reference line is determined by the significance level, which is set at 0.95. By applying the Pareto principle, it is possible to determine that a specific group of factors from the entire production process significantly influences the occurring issues. Investigated factors like model orientation and layer height affect the Rz roughness parameter but differ in the magnitude of their influence (Figs. 5, 6). Setting the orientation of the sample in the printing chamber represents the main difference in surface roughness values. The main cause is the layering of the input material and its subsequent solidification. The impact of the layer height parameter itself reinforces this. Based on the measured data, chamber temperature and laser power do not impact surface roughness (Fig.7).

The sample orientation plays a crucial role in determining the properties of parts produced by Selective Laser Sintering (Fig. 7). The layered build process inherent to SLS creates anisotropic behavior, meaning the mechanical and surface properties of the final part can vary significantly depending on its orientation within the build chamber. Surfaces facing upwards tend to have higher roughness due to the step effect inherent in layered manufacturing. Surfaces parallel to the build platform (orientation E) exhibit lower roughness with an Rz value in the range of 32 µm to 35 µm (Fig. 8). Samples oriented perpendicular to the platform, i.e., orientation A and M, have similar surface roughness results Rz, with values ranging from 34 µm to 37 µm. To better understand the impact of part orientation, it is important to evaluate additional mechanical properties such as tensile, flexural, and compressive strength, as well as hardness and impact resistance. Understanding how part orientation affects the overall mechanical performance is crucial for selecting the optimal orientation for specific applications. The experimental results demonstrate that layer height and part orientation are significant factors in determining the surface quality of PA12 parts produced by the Selective Laser Sintering process.

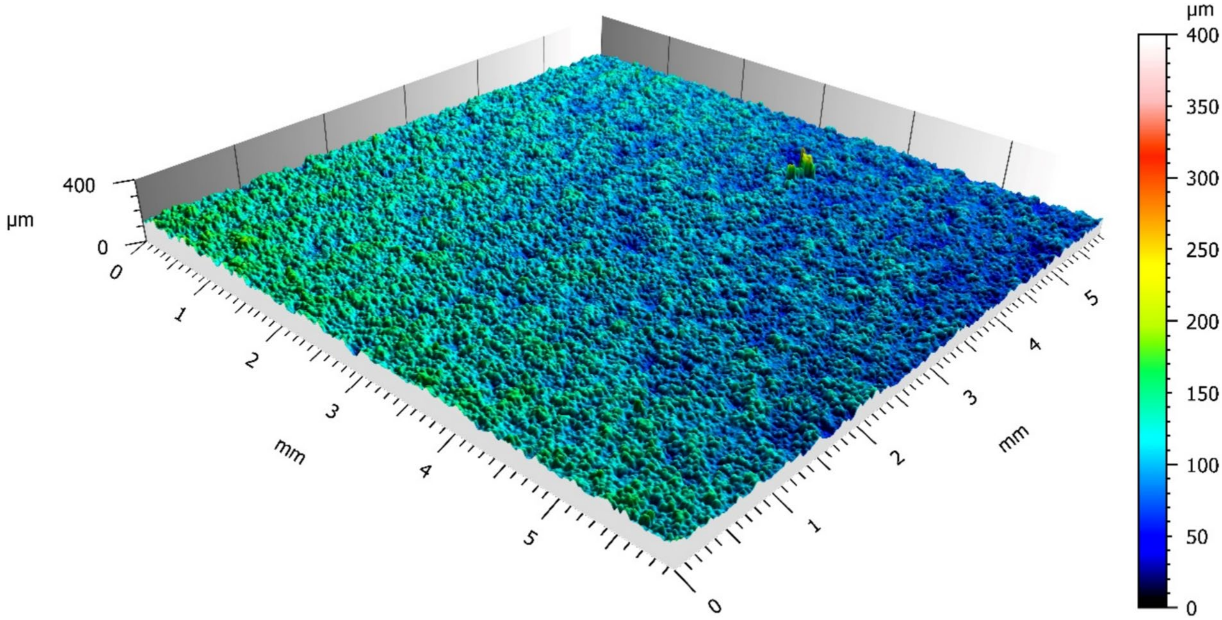


**Fig. 5** Topography of the specimen surface of experiment 5, orientation E

**Fig. 6** Topography of the specimen surface of experiment 5, orientation D

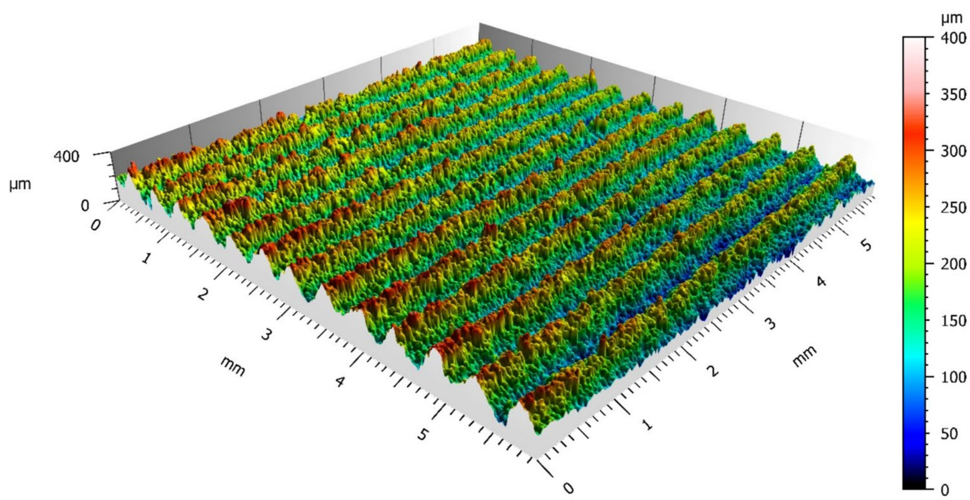


The base chamber temperature observed on the LISA device for the PA12 Smooth material is 178.5 °C, with the displayed temperature fluctuating within ± 0.5 °C. Higher laser power causes localized sintering of the powder material and leads to its overflow through individual layers. This material overflow and the resulting lower Rz roughness values can negatively impact the accuracy of manufactured parts and lead to detail loss. Furthermore, during production, it was noted that compensating the temperature by −1 °C resulted in the powder material remaining powdery after production. Moreover, the bottom base layers of the working chamber showed minimal burn marks on the working platform. However, when compensating for a temperature increase of + 2 °C, after production, the entire block of powder material exhibited greater cohesion, containing more clumps. At the same time, the bottom layers that came into contact with the working platform contained burnt spots, which are undesirable waste in SLS additive manufacturing.

The surface roughness parameter Rz data were statistically analyzed using Minitab software, and the presented model achieved a confidence level of 86.17%. Figure 9 illustrates the impact of layer height on surface roughness during SLS printing. The highest measured Rz roughness values were observed at a layer height of 0.175 mm, which was the maximum value investigated. The surface roughness parameter Rz ranged from 34.9 µm to 43.5 µm, with extremes of 29 µm to 53 µm. Comparable Rz roughness values were obtained at layer heights of 0.1 and 0.125 mm

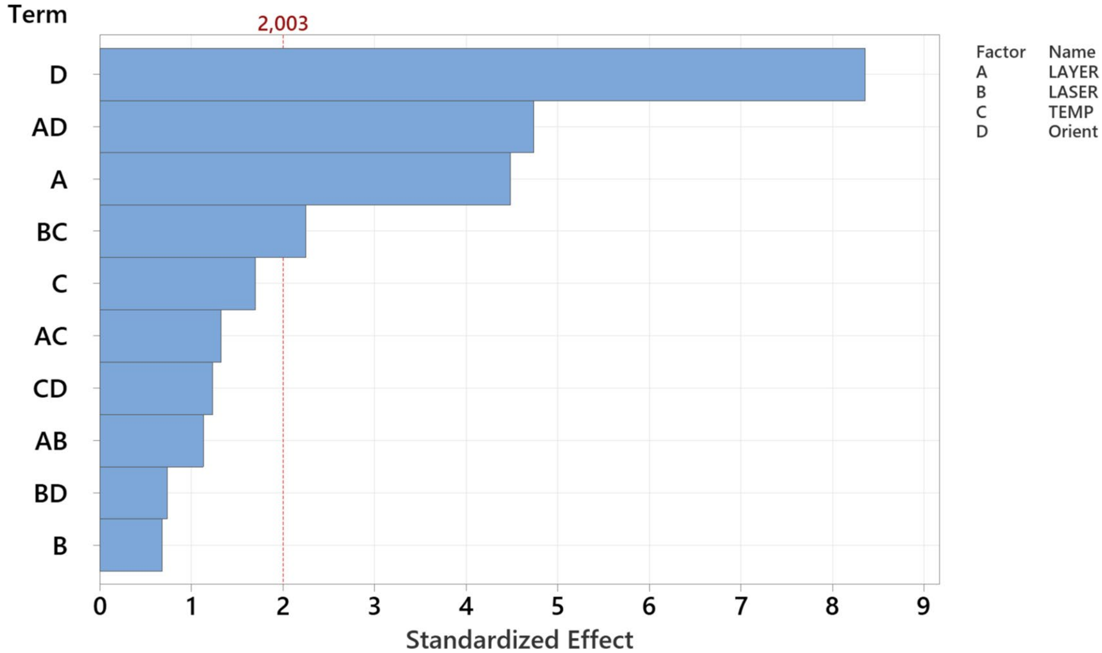


**Fig. 7** The effect of the selected parameters on the roughness Rz

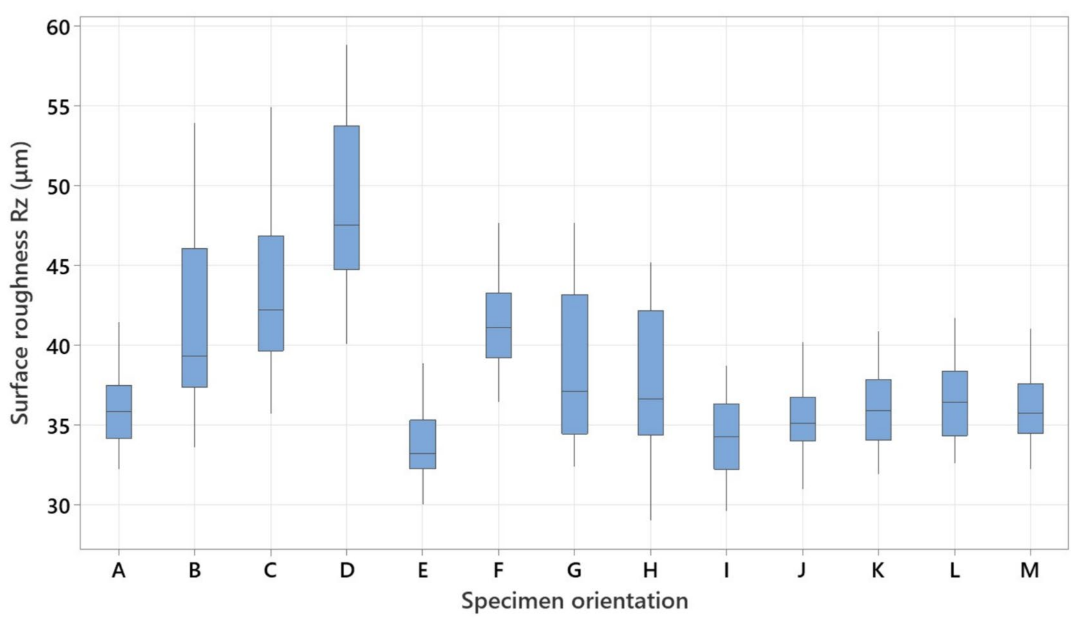


**Fig. 8** Effect of specimen orientation on roughness parameter Rz

with values 34 µm to 40 µm. It is noteworthy that the lowest layer setting of 0.1 mm is optimal for surface quality while simultaneously reducing laser power and increasing chamber temperature. This finding suggests that using a lower layer height setting can improve the surface quality of parts produced by the SLS printing process, which is a significant consideration for applications where surface finish is critical.

## 3.2 Mechanical properties

Mechanical testing was conducted based on tensile testing (ISO 527–1:2012). Using mathematical and statistical software Minitab, a data model was generated to evaluate the tensile strength of the PA12 Smooth material. The overall reliability of the tensile strength evaluation model

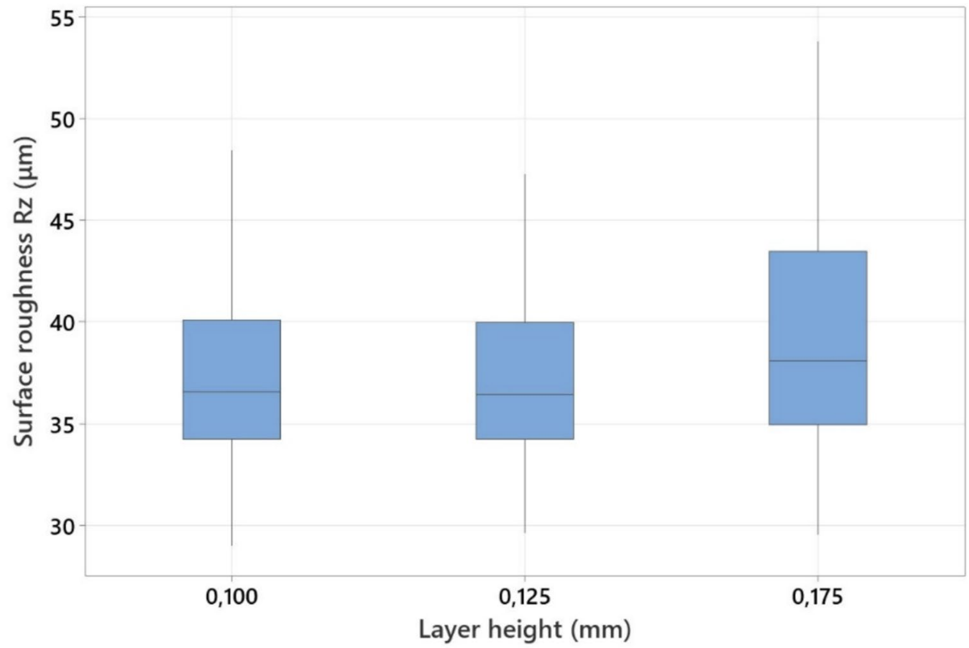


**Fig. 9** Effect of layer height on roughness parameter Rz

is 82.42%. For easier interpretation, the data were graphically processed.

The model orientation within the chamber of the SLS additive manufacturing device significantly influences the tensile strength. The obtained tensile strength values ranged from 19 MPa to a maximum of 49.05 MPa (Fig. 10), with extremes ranging from 9.9 MPa to a maximum of 53.4 MPa. Samples that oriented along the Z-axis (orientations A, B, L, M) exhibited the lowest tensile strengths. This is because the stress is perpendicular to the layer, leading to sample failure directly after each layer. On the contrary, samples in the XY plane (orientations E, F, G) showed tensile strengths exceeding the values provided by the material manufacturer. However, significant deformation occurred in samples in the XY plane (Fig. 11). This could be due to high thermal stress on individual layers during laser curing and subsequent cooling. This phenomenon could be mitigated by adjusting the cooling time of the device's working chamber. However, the basic version of Sinterit Studio has a preset cooling time and does not allow this parameter to be changed. Samples oriented at a 22.5° angle to the XY plane did not

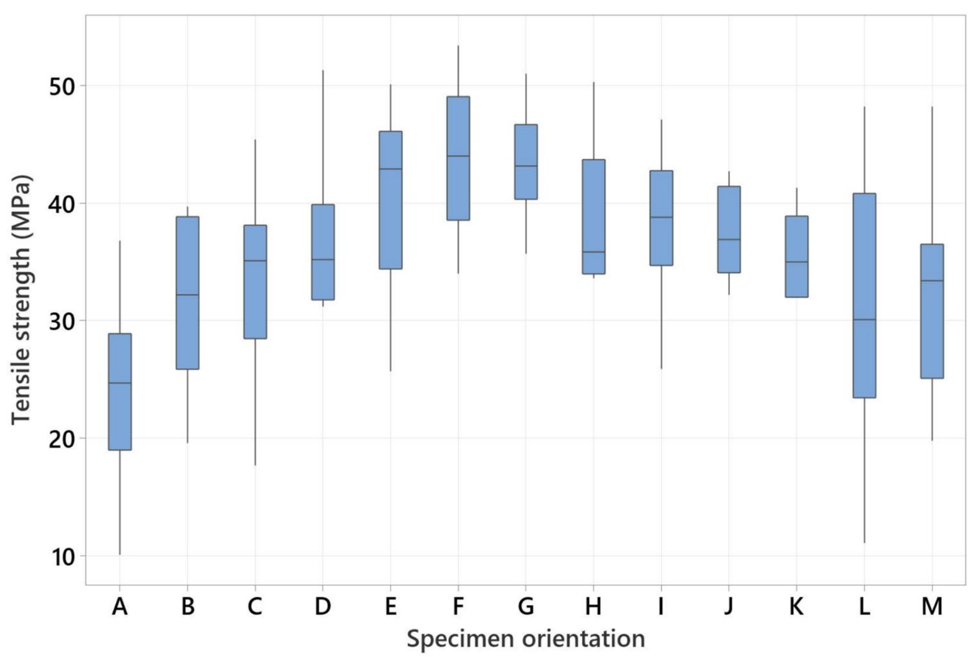


**Fig. 10** Effect of orientation on tensile strength


**Fig. 11** Comparison of deformed specimens and specimens without deformation

exhibit deformation, and their tensile strength ranged from 38.2 MPa to 39.3 MPa. The tensile strength specified by the manufacturer for PA12 Smooth material is set at 38 to 42 MPa.

The laser power and chamber temperature have a significant effect on the strength of the samples. These parameters are crucial factors in the sintering process during SLS additive manufacturing. While the chamber temperature serves to preheat the material, the laser power directly influences the sintering of the powder material to form a solid structure. The experimental data show that higher laser power and increased chamber temperature (Fig. 12) lead to higher tensile strength values. Increasing the energy input during sintering leads to improved bonding between individual layers, consequently enhancing the strength of the products. However, an undesired effect can be the occurrence of deformation due to rapid cooling and loss of details, as the material sintering can cause the edges to round, which was observed on the embedded text labeling the individual samples.

Our findings indicate a strong relationship between SLS process parameters (temperature compensation and laser power ratio) and the resulting tensile strength of specimens. A temperature compensation of + 2 °C and a laser power ratio of 1.6 yielded the highest tensile strengths (40.6 MPa to 50.8 MPa). Conversely, a temperature compensation of −1 °C and a laser power ratio of 0.8 resulted in significantly lower and more dispersed tensile strengths (12 MPa to 34 MPa).

The large dispersion at the −1 °C and 0.8 laser power ratio suggests that these settings may lead to inconsistent melting and bonding of the PA12 powder. This could be

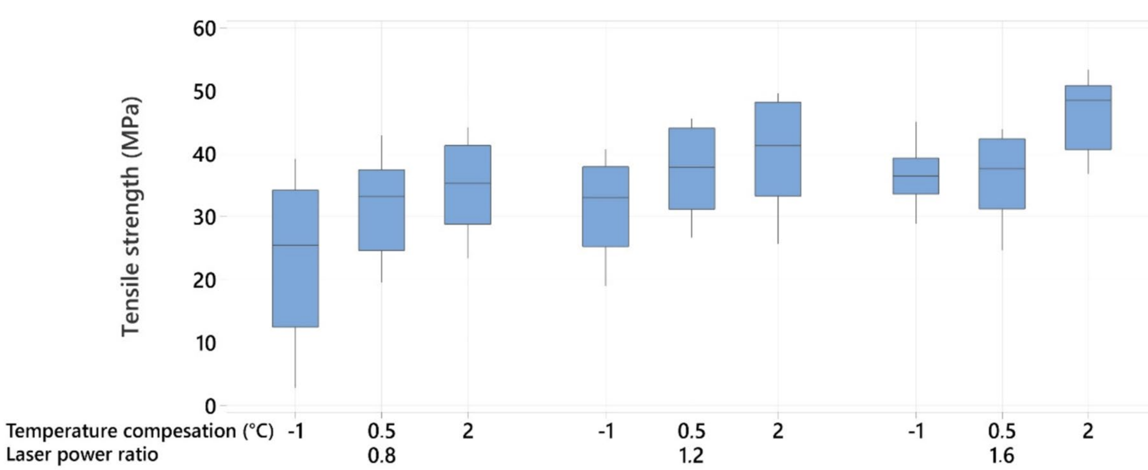


**Fig. 12** Effect of temperature compensation and laser power on tensile strength

due to insufficient energy input, leading to variations in part density and porosity. The higher and more consistent tensile strengths were observed at + 2 °C and 1.6 laser power ratio indicate more complete melting and better inter-particle bonding.

### 3.3 Geometric properties

In statistics, response surface methodology (RSM) examines relationships between multiple explanatory variables and one or more response variables. RSM is an empirical model that uses mathematical and statistical techniques to connect input factors with response. The main objective of RSM is to identify the impact of input variables that affect the outcome.

The investigated input factors and their interaction indicate that the roundness of the measured samples is influenced by the model orientation in the chamber and the laser power of the SLS device (Fig. 13). The accuracy of the mathematical-statistical regression model reached 96.03%. The impact of chamber temperature and layer height on cylindricity was examined, but their impacts were found insignificant. The largest absolute deviations in roundness were recorded with orientation C, where the sample was oriented at a 45° angle (Fig. 14). Roundness deviations ranged from an absolute value of 0.265 mm to 0.523 mm. Furthermore, the roundness deviations showed an increasing trend with increasing laser power, and their range expanded. The highest absolute range was observed at a laser power of 1.6, where the absolute roundness deviation values ranged from 0.174 mm to 0.523 mm.

A visual comparison for four differently oriented samples made under the experimental parameters 2 and 7 is depicted in Fig. 15. The sample from experiment 2, oriented in position E (2CFE), where the axis of the cylindrical part is perpendicular to the XY plane of the manufacturing chamber, displayed a roundness deviation of 0.08 mm. Upon changing the sample orientation to position C (2CFC), indicating a 45° tilt to the XY plane, a significant shape change occurred, with the roundness deviation reaching 0.243 mm. Deviations in samples 2CFC and 7CFC did not exhibit a symmetric pattern; they were unevenly directed away from the nominal value. Notably, in samples 2CFE and 7CFE, opposite measured sections displayed the same direction. Thus, within the measured ranges of 40°–90° and 200°–260°, the roundness deviation was negative from the nominal shape, while in the range of 290°–20° and 100°–190°, the deviation was positive. Deformation caused by the weight load of samples, which would impact objects above them in the manufacturing chamber, can be discounted in orientation E, as the axis of the cylindrical part is perpendicular to the XY plane, ensuring any weight load acts perpendicularly to the measured roundness elements. Samples 2CF were produced under process parameters where the laser power ratio reached its highest value, at 1.6. Chamber temperature regulation was set at + 2 °C, consistent across setting 7 (7CFE,

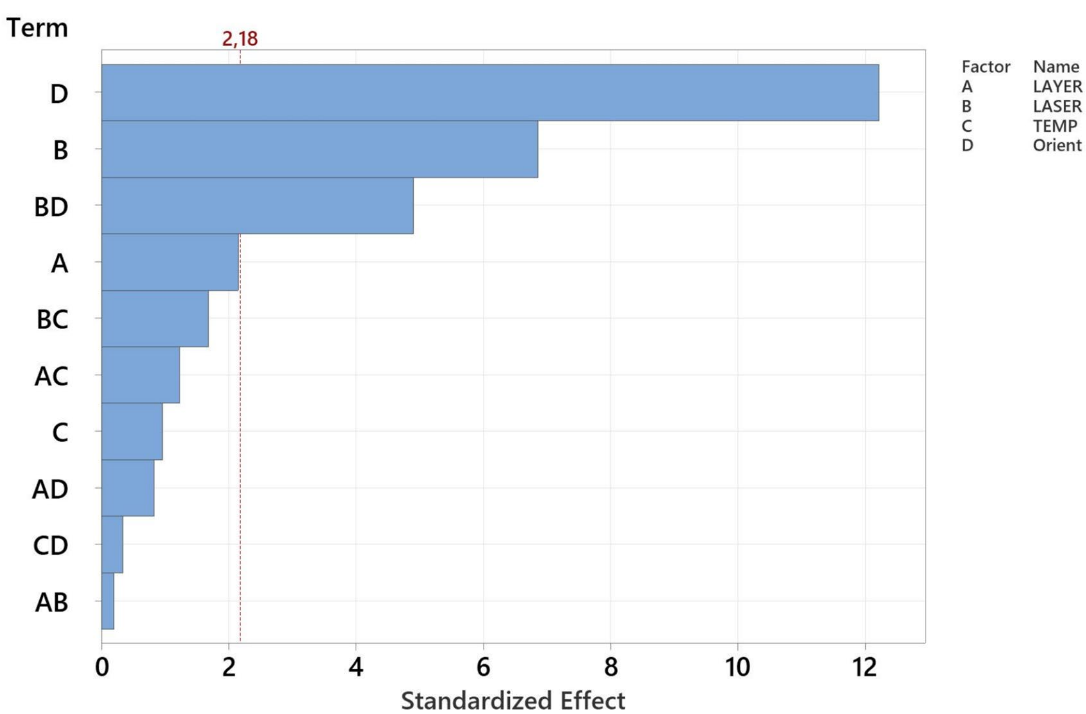


Fig. 13 The effect of the selected parameters on the roundness

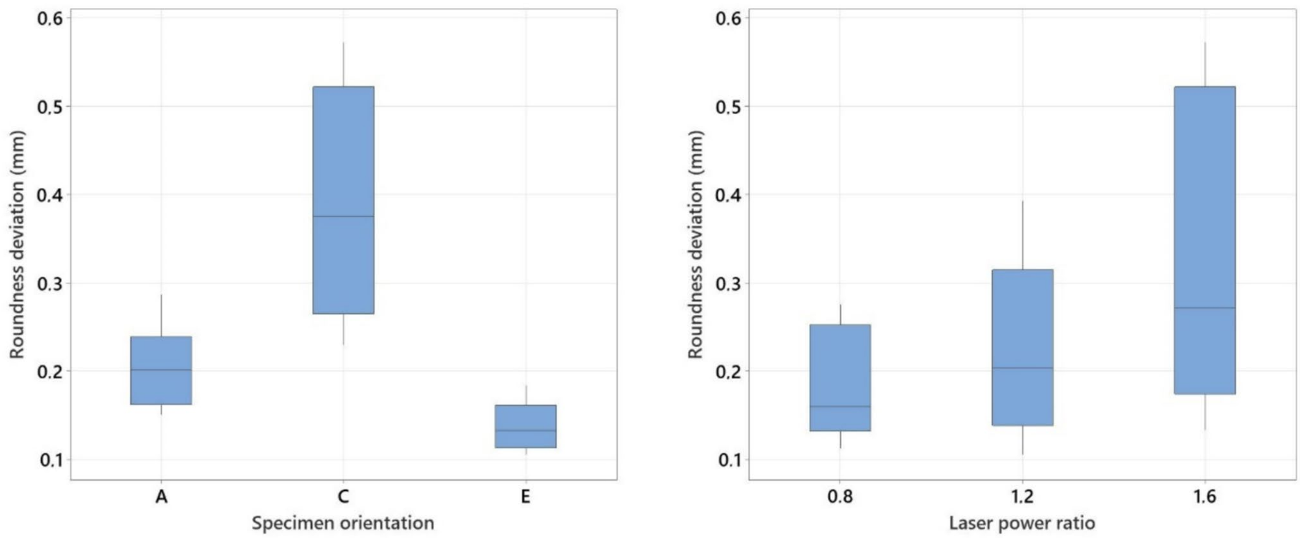


**Fig. 14** Roundness deviation in the investigated orientations and laser power ratio

7CFC). However, in this setting, it is important to note that the laser power was at a minimum value of 0.8. The roundness deviation for sample 7CFE was 0.087 mm, while for position C, it was 0.238 mm.

The main factor contributing to variations in roundness depending on sample orientation is the shape of the sample cross-section at the manufacturing layer. When the sample axis is perpendicular to the XY plane, the laser-solidified layer assumes a circular shape, meaning that roundness deviation is directly affected by the laser accuracy in the XY plane. However, when the sample is angled, the layers are not solidified in a circular shape but in an inclined cut, determined by the angle rotation relative to the XY plane.

### 3.4 Dimensional accuracy

Dimensional accuracy was evaluated by conducting CMM measurements of the diameters of all circular artifacts by the STN EN ISO ASTM 52902:2019 standard. The measurements were conducted on the inner or outer circumference, depending on the analyzed element to ensure accurate data collection. All investigated parameters affected the achieved part accuracy (Fig. 16). Analysis of the dimension measurements revealed a significant impact of laser power on dimensional accuracy. Additionally, layer height and chamber temperature were found to be influential parameters. While the model orientation did have a statistical impact, its significance in terms of magnitude was minimal. The accuracy of the regression model R-sq reached 96.39%.

The deviation range from the diameter is illustrated in Fig. 17. The most significant deviations from the diameter occurred at a laser power setting of 1.6, the highest value investigated. These deviations varied notably based on the size and type of the diameter, whether it was an outer or inner diameter. Positive deviations were consistently noted on all outer diameters, their extent influenced by the 3D printing process parameters. Conversely, the inner circles predominantly exhibited negative deviations. While the parameters affected their size, their deviation nature remained consistent. The highest deviation values were registered at a laser power of 1.6, with maximum deviations of + 0.63 mm on the circle with a diameter of ⌀ 23.5 mm and + 0.67 mm on the circle with a diameter of ⌀ 8 mm. Negative deviations of -0.83 mm were recorded on the inner circles with a diameter of ⌀ 15 mm and a deviation of -0.68 mm on the circle with a diameter of ⌀ 7 mm.

The effect of individual parameters is depicted in Fig. 18. As the values of the investigated factors, such as layer height, laser power, and chamber temperature increased, dimensional deviations increased, too. Therefore, we should consider their impact on dimensional accuracy to find the optimal settings to achieve the desired accuracy based on the required properties. The lowest deviations from the nominal dimension could be achieved by setting the process parameters to a layer height of 0.1 mm, laser power of 0.8, and adjusting the chamber temperature offset by + 2 °C.

## 4 Discussion

Additive manufacturing has become a significant technology in modern industry, enabling the creation of complex geometric structures layer by layer. One of the additive manufacturing methods is Selective Laser Sintering (SLS), whose popularity is increasing due to its ability to produce intricately shaped and functional parts from various materials.

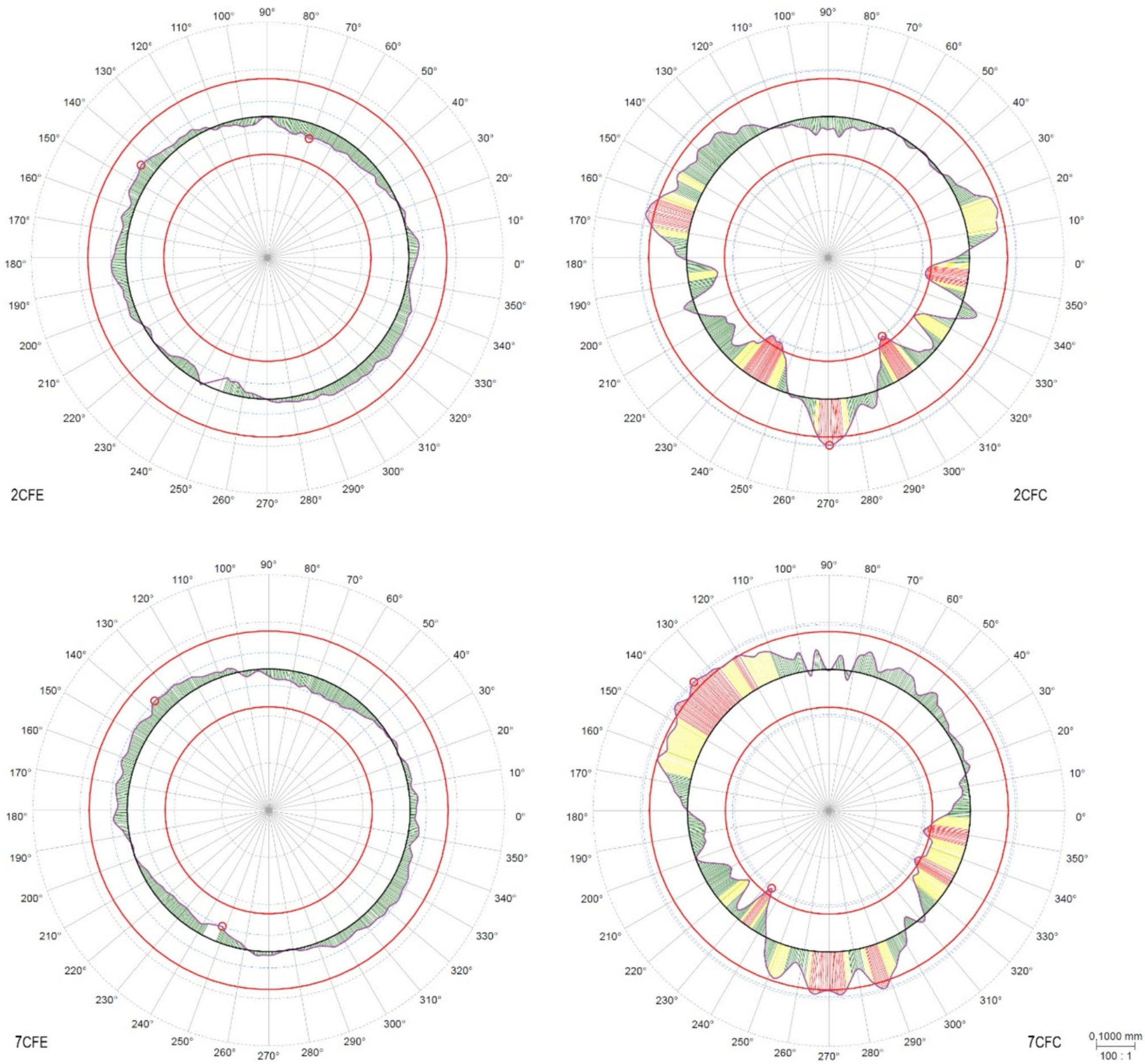


**Fig. 15** Visual representation of measured specimens 2CFE, 2CFC, 7CFE, 7CFC

In this study, we investigated the impact of process parameters in the Selective Laser Sintering additive technology on the properties of printed samples, focusing on tensile strength, roundness, surface roughness, and dimensional accuracy. Our analysis of experimental results provides valuable insights into the SLS process.

Our interpretation of the results confirmed our hypothesis that process parameters significantly affect the properties of the printed samples. We found that changes in parameters such as layer height, laser power, chamber temperature, and sample orientation lead to significant changes in the properties of printed objects. The most significant change was observed in tensile strength, as increases in laser power, chamber temperature, and model orientation led to higher material strength as the powder particles transformed under higher laser energy, fusing and increasing part strength. This claim is consistent with the findings of Razaviye [20]. On the contrary, lower chamber temperatures and inappropriate sample positioning can decrease the strength. The difference in tensile strength shows high disparities depending on sample orientation, with samples in the XY plane achieving the highest strength. These results corroborate the study by Calignano, although it should be noted that their research focused only on two orientations, 0° and 90°, which may be insufficient for SLS production [42]. Regarding the roundness of samples, we observed a significant impact of model orientation,

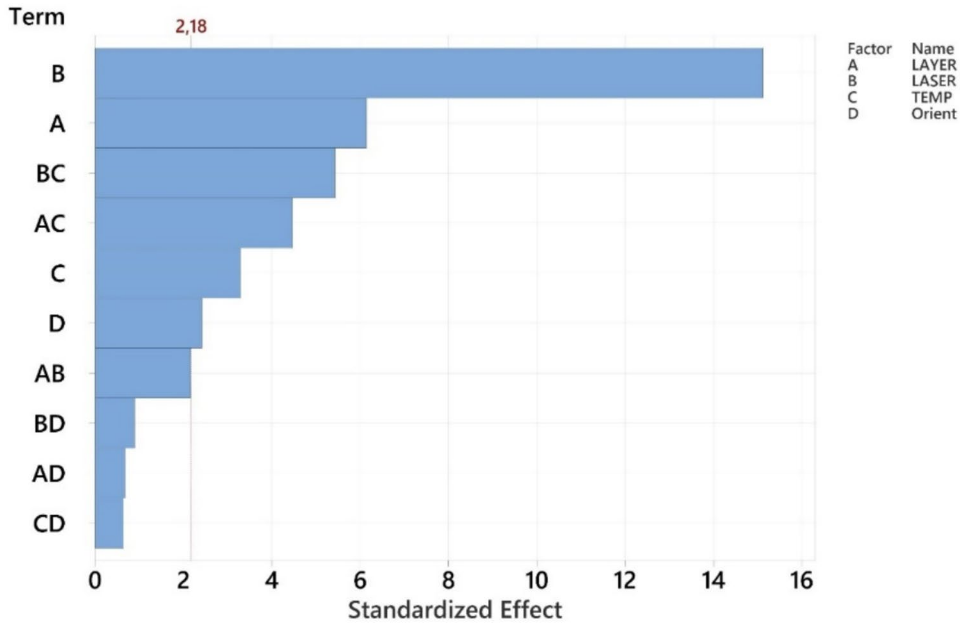


**Fig. 16** The effect of the selected parameters on the dimensional accuracy

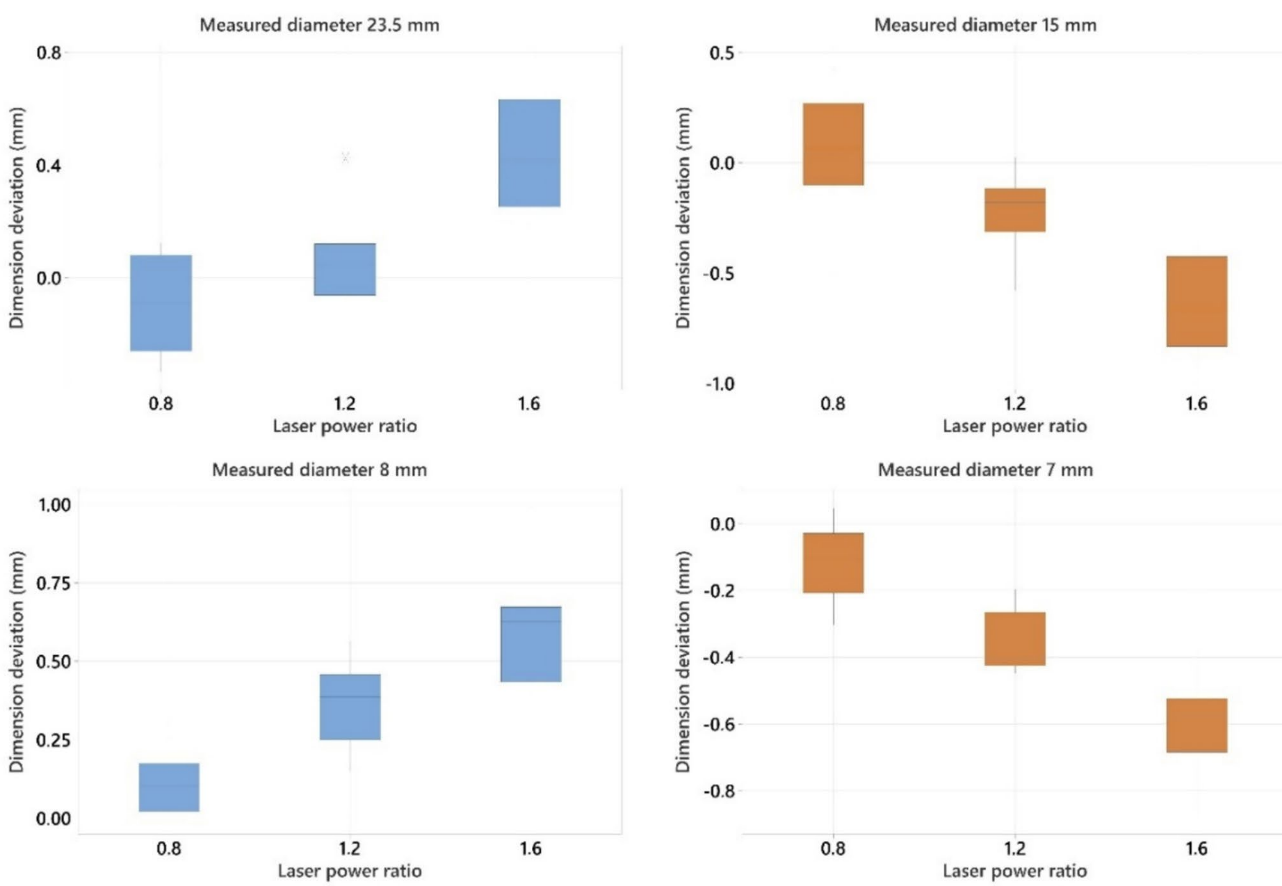


**Fig. 17** The deviation range from the measured diameter

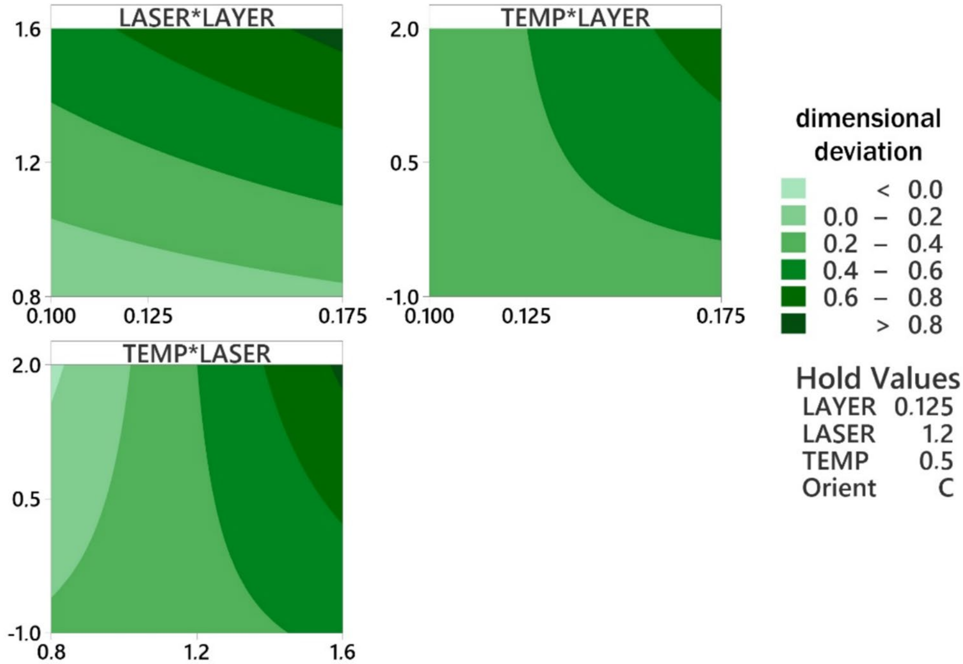


**Fig. 18** Effect of parameters on dimensional deviation

where changes in rotation relative to the XY plane affect the geometric accuracy of manufactured objects. Although rotation by 30°–45° increases roundness deviations, it has positive results in terms of tensile strength. Surface roughness was not significantly affected by laser power and chamber temperature. While higher values of these parameters resulted in lower surface roughness, the reduction was only up to 2.5 µm for the Rz roughness parameter, whereas layer height caused a 5 µm change. Achieved Rz roughness values ranged from 35.5 to 40 µm. For comparison, Sachdeva achieved similar results after optimizing the SLS process [16].

The limitation of this study is that only one material, PA12, was used and specific settings on the Sinterit Lisa printer. Other materials and other types of additive manufacturing equipment should be considered in future research work to get a wider perception of the SLS process. The strong recommendation for further research is focused on the process parameters in the search for improved properties of the printed objects. We can also envision applications of our findings in industrial sectors such as automotive, aerospace, or medical industries, where high print quality and mechanical material properties are crucial. Generally, our study provides valuable insights for engineering practice and development in 3D printing using the SLS method and promotes further research within this scope.

## 5 Conclusion

The presented work focused on the additive technology of SLS and its fundamental process parameters for printing material PA12. Understanding the impact of factors is essential for properly setting up manufacturing equipment to achieve the desired quality of produced parts. Parameters such as laser power, layer height, chamber temperature, and model orientation in the chamber are fundamental to SLS technology. Their impact was examined in terms of achieved surface roughness, tensile strength, geometric roundness properties, and dimensional accuracy. The values of the examined factors were chosen based on the parameters of the SLS device and its control program. The device used is the affordable, compact-sized Sinterit Lisa, often used in the initial implementation of additive manufacturing in industries. Its manufacturing capacity is appropriate for beginners, and its setup options correspond to this. Its control and slicing program, Sinterit Studio Basic, allows setting only three selected process parameters, with the disadvantage that some factors can only be adjusted in terms of the offset to the selected printing material. From the experimental measurements and gained data, we can confirm that:

- The quality of the resulting print is directly affected by the settings of laser power, layer height, and chamber temperature, and it is fundamentally affected by the orientation and rotation of the model itself.
- Model orientation significantly affects the tensile strength of parts. To achieve higher strength, enlarge the area of the burned material layer and rotate the model so that the load force runs parallel to the layers. To optimize tensile strength, the model should be positioned at a 22.5° angle from the XY plane, as shown with specimens D and J, which experienced no deformation.

- When positioning the model, it is necessary to consider the risk of undesirable thermal deformation. More thermal energy, delivered by higher laser power and chamber temperature, results in better material strength. As the model rests in the XY plane, specimens E, F, and G face the looming threat of thermal deformation.
- The increase in laser power and chamber temperature does not significantly impact surface roughness. However, the Rz roughness parameter is sensitive to layer height and orientation, with the lowest values at a model orientation parallel to the XY plane and lower layer heights. The optimal lowest layer setting of 0.1 mm ensures better surface quality when the model orientation is set to 22.5° to the XY plane.
- The roundness of measured specimens is significantly influenced by model orientation, while the dimensional accuracy of measured diameters depends on laser power. To achieve a low roundness value, the model must be oriented so that its circular cross-section is in the XY plane or perpendicular to this plane (specimens A, E).
- Each observed parameter in this study influences a specific aspect of the quality of the manufactured part output. Therefore, the process parameters should be chosen carefully to achieve the desired quality. Model orientation impacts the quality most significantly during printing and should be carefully considered in SLS additive manufacturing.

This research has the potential to contribute to further advancements in additive manufacturing. Furthermore, it provides a foundation for future experiments to optimise the SLS process for various industrial and mechanical engineering applications.

**Acknowledgements** The article was supported by the grant scheme APVV-23-0366: "Research of reference standards and measurement methods ensuring determination of the relationship of geometric specifications and qualitative indicators of 3D objects created by additive technologies", APVV-22-0328: " Design of a Methodology and its Verification for the Measurement of Selected Parameters of Ti Implants in the Manufacturing Process", APVV-20-0561: " Research on the implementation of new measurement methods for the calibration of measurement systems for industrial metrology practice".

**Author contributions** Richard Joch: writing—review and editing, writing—original draft, visualization, validation, software, resources, methodology, investigation, conceptualization, data curation. Michal Šajgalík: writing—review and editing, supervision, methodology, data curation. Mário Drbúl: validation, software, methodology, investigation, resources, project administration. Dagmar Měřínska: validation, software, resources, methodology, data curation. Jaromír Markovič: supervision, resources, project administration, investigation, and funding acquisition. Andrej Czán: methodology, resources, project administration, investigation, and funding acquisition.

**Funding** Open access funding provided by The Ministry of Education, Science, Research and Sport of the Slovak Republic in cooperation with Centre for Scientific and Technical Information of the Slovak Republic. Agentúra na Podporu Výskumu a Vývoja, APVV-22-0328, MARKOVIČ Jaromír, APVV-20-0561, CZÁN Andrej, APVV-23-0366, DRBÚL Mário.

**Data availability** Data will be made available on request.

## Declarations

**Conflict of interest** The authors declare that they have no known competing financial interests or personal relationships that could have appeared to influence the work reported in this paper.



## References

1. Wong KV, Hernandez A (2012) A review of additive manufacturing. ISRN Mech Eng 2012:1–10. https://doi.org/10.5402/2012/208760
2. Dizon JRC, Espera AH, Chen Q, Advincula RC (2018) Mechanical characterization of 3D-printed polymers. Addit Manuf 20:44–67. https://doi.org/10.1016/J.ADDMA.2017.12.002
3. O'Connor HJ, Dowling DP (2020) Comparison between the properties of polyamide 12 and glass bead filled polyamide 12 using the multi jet fusion printing process. Addit Manuf 31:100961
4. Martynková GS, Slíva A, Kratošová G et al (2021) Polyamide 12 materials study of morpho-structural changes during laser sintering of 3d printing. Polymers (Basel) 13:810. https://doi.org/10.3390/polym13050810
5. Beniak J, Krizan P, Matus M (2020) Conductive material properties for fdm additive manufacturing. MM Sci J 2020:3846–3851
6. Beniak J, Holdy M, Križan P, Matúš M (2019) Research on parameters optimization for the Additive Manufacturing process. Transport Res Procedia 40:144–149. https://doi.org/10.1016/J.TRPRO.2019.07.024
7. Beniak J, Šooš L, Križan P et al (2022) Resistance and Strength of Conductive PLA Processed by FDM Additive Manufacturing. Polymers (Basel). https://doi.org/10.3390/polym14040678
8. Chacón JM, Caminero MA, García-Plaza E, Núñez PJ (2017) Additive manufacturing of PLA structures using fused deposition modelling: Effect of process parameters on mechanical properties and their optimal selection. Mater Des 124:143–157. https://doi.org/10.1016/j.matdes.2017.03.065
9. Waseem M, Salah B, Habib T et al (2020) Multi-response optimization of tensile creep behavior of PLA 3D printed parts using categorical response surface methodology. Polymers (Basel) 12:1–16. https://doi.org/10.3390/polym12122962

10. Rabinowitz A, DeSantis PM, Basgul C et al (2023) Taguchi optimization of 3D printed short carbon fiber polyetherketoneketone (CFR PEKK). J Mech Behav Biomed Mater. https://doi.org/10.1016/j.jmbbm.2023.105981
11. Reber R, Koo B, Liu D (2019) Polyetherketoneketone (PEKK), a versatile ultra-polymer for additive manufacturing. In: International SAMPE Technical Conference
12. Kishore V, Chen X, Ajinjeru C, et al (2016) Additive manufacturing of high performance semicrystalline thermoplastics and their composites. In: Solid Freeform Fabrication 2016: Proceedings of the 27th Annual International Solid Freeform Fabrication Symposium - An Additive Manufacturing Conference, SFF 2016. pp 906–915
13. Majko J, Vaško M, Handrik M, Sága M (2022) Tensile properties of additively manufactured thermoplastic composites reinforced with chopped carbon fibre. Materials. https://doi.org/10.3390/ma15124224
14. Ngo TD, Kashani A, Imbalzano G et al (2018) Additive manufacturing (3D printing): a review of materials, methods, applications and challenges. Compos B Eng 143:172–196. https://doi.org/10.1016/j.compositesb.2018.02.012
15. Olejarczyk M, Gruber P, Ziółkowski G (2020) Capabilities and limitations of using Desktop 3-D printers in the laser sintering process. Appl Sci (Switzerland). https://doi.org/10.3390/APP10186184
16. Sachdeva A, Singh S, Sharma VS (2013) Investigating surface roughness of parts produced by SLS process. Int J Adv Manuf Technol 64:1505–1516. https://doi.org/10.1007/s00170-012-4118-z
17. Faraj Z, Aboussaleh M, Zaki S et al (2022) Optimization of the parameters of the selective laser sintering for the formation of PA12 samples by the Taguchi method. Int J Adv Manuf Technol 122:1669–1677. https://doi.org/10.1007/s00170-022-09991-7
18. Negi S, Dhiman S, Sharma RK (2014) Investigating the Surface Roughness of SLS Fabricated Glass-Filled Polyamide Parts Using Response Surface Methodology. Arab J Sci Eng 39:9161–9179. https://doi.org/10.1007/s13369-014-1434-7
19. Nar K, Majewski C, Lewis R (2022) A comprehensive characterisation of Laser Sintered Polyamide-12 surfaces. Polym Test 106:107450. https://doi.org/10.1016/j.polymertesting.2021.107450
20. Razaviye MK, Tafti RA, Khajehmohammadi M (2022) An investigation on mechanical properties of PA12 parts produced by a SLS 3D printer: An experimental approach. CIRP J Manuf Sci Technol 38:760–768. https://doi.org/10.1016/J.CIRPJ.2022.06.016
21. Gadelmoula A, Aldahash SA (2023) Tribological properties of glass bead-filled polyamide 12 composite manufactured by selective laser sintering. Polymers (Basel). https://doi.org/10.3390/polym15051268
22. Petzold S, Klett J, Schauer A, Osswald TA (2019) Surface roughness of polyamide 12 parts manufactured using selective laser sintering. Polym Test. https://doi.org/10.1016/j.polymertesting.2019.106094
23. DincăShamieh LL, Popa NM, Milodin NL et al (2019) Influence of the process parameters on mechanical properties of the final parts obtained by selective laser sintering from PA2200 powder. MATEC Web Conf 299:01001. https://doi.org/10.1051/mateconf/201929901001
24. Shi Y, Li Z, Sun H et al (2004) Effect of the properties of the polymer materials on the quality of selective laser sintering parts. Proceed Instit Mech Eng, Part L: J Mater: Design Appl. https://doi.org/10.1243/1464420041579454
25. Averardi A, Cola C, Zeltmann SE, Gupta N (2020) Effect of particle size distribution on the packing of powder beds: A critical discussion relevant to additive manufacturing. Mater Today Commun. https://doi.org/10.1016/j.mtcomm.2020.100964
26. Galati M, Calignano F, Defanti S, Denti L (2020) Disclosing the build-up mechanisms of multi jet fusion: Experimental insight into the characteristics of starting materials and finished parts. J Manuf Process 57:244–253. https://doi.org/10.1016/J.JMAPRO.2020.06.029
27. Zarringhalam H, Hopkinson N, Kamperman NF, de Vlieger JJ (2006) Effects of processing on microstructure and properties of SLS Nylon 12. Mater Sci Eng, A 435–436:172–180. https://doi.org/10.1016/j.msea.2006.07.084
28. Dadbakhsh S, Verbelen L, Verkinderen O et al (2017) Effect of PA12 powder reuse on coalescence behaviour and microstructure of SLS parts. Eur Polym J 92:250–262. https://doi.org/10.1016/j.eurpolymj.2017.05.014
29. Feng L, Wang Y, Wei Q (2019) PA12 powder recycled from SLS for FDM. Polymers (Basel). https://doi.org/10.3390/polym11040727
30. Vendittoli V, Gazzerro A, Polini W, Sorrentino L (2023) Dimensional and geometric deviations of parts in PA12 manufactured by selective laser sintering: numerical and experimental analyses. In: Materials Research Proceedings. pp 198–205
31. Uddin M, Williams D, Blencowe A (2021) Recycling of selective laser sintering waste Nylon powders into fused filament fabrication parts reinforced with Mg particles. Polymers (Basel). https://doi.org/10.3390/polym13132046
32. Sillani F, Kleijnen RG, Vetterli M et al (2019) Selective laser sintering and multi jet fusion: Process-induced modification of the raw materials and analyses of parts performance. Addit Manuf 27:32–41. https://doi.org/10.1016/J.ADDMA.2019.02.004
33. He B-F, Ding S-Y, Wei C-E et al (2019) Review of measurement methods for areal surface roughness | 三维表面粗糙度测量方法综述. Guangxue Jingmi Gongcheng/Optics Precision Eng 27:78–93. https://doi.org/10.3788/OPE.20192701.0078
34. Liu C, Lu R, Chen L, Wang J (2010) Progress of surface roughness measurement based on optical method. Bandaoti Guangdian/Semiconductor Optoelectronics 31:495–500
35. Kozior T, Bochnia J, Bochenek A et al (2024) Estimating the Uncertainty of Measurements for Various Methods and 3D Printed Parts. Appl Sci (Switzerland). https://doi.org/10.3390/app14083506
36. Gong Y, Xu J, Buchanan RC (2019) Surface roughness: A review of its measurement at micro-/nano-scale. Phys Sci Rev. https://doi.org/10.1515/psr-2017-0057
37. Shao M-Q, Xu D, Li S-Y et al (2023) A review of surface roughness measurements based on laser speckle method. J Iron Steel Res Int 30:1897–1915. https://doi.org/10.1007/s42243-023-00930-8
38. Lisa_specification. https://sinterit.com/wp-content/uploads/2022/02/Lisa_specification_v2.pdf. Accessed 9 Dec 2024
39. Krupova H, Sternadelova K, Mesicek J et al (2024) Experimental evaluation of selectively laser sintered polyamide 12 surface treatment for direct electrodeposition. Prog Org Coat. https://doi.org/10.1016/j.porgcoat.2023.107968
40. Zárybnická L, Petrů J, Krpec P, Pagáč M (2022) Effect of Additives and Print Orientation on the Properties of Laser Sintering-Printed Polyamide 12 Components. Polymers (Basel). https://doi.org/10.3390/polym14061172
41. Sinterit PA12 Smooh. https://sinterit.com/materials/pa12-smooth/. Accessed 10 Dec 2024
42. Calignano F, Giuffrida F, Galati M (2021) Effect of the build orientation on the mechanical performance of polymeric parts produced by multi jet fusion and selective laser sintering. J Manuf Process 65:271–282. https://doi.org/10.1016/j.jmapro.2021.03.018